

# Application of DRM-Trefftz and DRM-MFS to Transient Heat Conduction Analysis

Leilei Cao<sup>1,2</sup>, Qing-Hua Qin<sup>\*2</sup> and Ning Zhao<sup>1</sup>

<sup>1</sup>*School of Mechatronics, Northwestern Polytechnical University, Xi'an 710072, P.R. China*

<sup>2</sup>*Department of Engineering, Australian National University, Canberra, ACT 0200, Australia*

**Abstract:** In this article we present two numerical models for solving transient heat conduction problems. One is based on dual reciprocity method and Trefftz method (dubbed DRM-Trefftz), and the other is based on dual reciprocity method and fundamental solution (dubbed DRM-MFS). A time stepping method is used in handling the time variable to convert the problem into a set of inhomogeneous modified Helmholtz equations. The solution of the modified Helmholtz equation is divided into two parts, i.e. the particular solution and the homogeneous solution. While the particular solution is solved by DRM in which the source term is approximated by radial basis functions (RBF), the homogeneous solution is obtained by using MFS or Trefftz method. Two types of bases functions, Trefftz solution and Fundamental solution are used to approximate the homogeneous solution. The proposed two meshless methods require only discrete nodes constructed on domain and boundary. Finally, the parameters that influence the performance of the proposed method are assessed through several numerical examples. The results are presented for illustrating the accuracy and efficacy of the proposed numerical models.

**Keywords:** Transient heat conduction, dual reciprocity method, fundamental solution, Trefftz function.

## 1. INTRODUCTION

During the past decades, lots of new advanced materials and technologies have been developed and used in aerospace technology and engineering, such as functionally graded materials [1] (FGM) and shaped memory alloy (SMAs), which are used as thermal barrier coating in high-temperature turbine engine (see patent [2, 3]) and telescopic wing system (see patent [4, 5]), respectively. Since the material like FGM and SMA are always working under tough temperature environment in aerospace, so it is necessary to know the thermal properties of these materials and thermal performance of the corresponding structures. Therefore, transient heat conduction analysis plays an important role in many fields of space technology and engineering.

On the other hand, various numerical models were developed for analyzing transient heat conduction problems [6-11] during the past years, such as Finite Element Method (FEM), Finite Difference Method (FDM) and Boundary Element Method (BEM). Among the above methods, FDM and FEM critically depend on the quality of mesh; however, generating a good quality of mesh for complicated geometry can be time-consuming. BEM involves only discretization of the boundaries which is an important advantage over FEM and FDM. However, the classical use of BEM for transient fields [12], based on discretization in time, usually results in domain integrals which may increase computing time and even cause some numerical problems and make BEM

relatively inefficient compared to FEM and FDM. The Dual Reciprocity Method [13] (DRM) offers a solution method to avoid domain integration and hence became very popular recently. In particular, the dual reciprocity boundary element method (DRBEM), which transforms domain integrals to the boundary integrals by combining radial basis functions and conventional BEM, has wide applications in practical engineering. Applications of this approach to transient heat conduction problems can be found in [10, 14-16]. The multiple reciprocity boundary element method (MRBEM) has been emerging as a promising method for handling domain integrals [17]. However, DRBEM and MRBEM require more sophisticated mathematical procedures and the EEM itself involves further numerical integrations with a singular integral.

Alternatively, an attractive option is the meshless discretization approach which has received considerable attention by mathematicians and engineers in recent years. Meshless methods only use a number of nodes scattered within the problem domain and on the boundary. Among the existing meshless methods, the techniques most commonly used are the method of fundamental solutions (MFS) [18-21] and methods based on the radial basis functions (RBF) [22-24]. The classical MFS is based on the approximation of the solution of a Boundary Value Problem (BVP) by a linear combination of fundamental solutions to the corresponding differential operator. The boundary conditions are then fitted by solving the linear system formed using a number of a collocation points. The singularities are avoided by the use of virtual boundaries outside the problem domain. The MFS is also known as the superposition method [25] and charge simulation method [26]. However, MFS has its limitation in that it can only solve homogeneous problems. The combination of MFS and RBF enables one to extend MFS to

\*Address correspondence to this author at the Department of Engineering, College of Engineering and Computer Science, The Australian National University, Canberra, ACT 2601, Australia; Tel: +61 2 6125 8274; Fax: +61 2 6125 0506; E-mail: qinghua.qin@anu.edu.au

non-homogeneous problems and various types of time-dependent problems [11, 27].

In contrast to the MFS which is based on the fundamental solution, the Trefftz method is formulated using the family of T-complete functions which are homogeneous solutions for the governing equation. The Trefftz method was initiated in 1926 [28]. Since then, it has been studied by many researchers (Cheung *et al.* [29, 30], Zielinski [31], Qin [32, 33], Kita [34]). Unlike in the method of fundamental solution which needs source points to be placed outside the domain in order to avoid singularity, T-complete functions are non-singularity inside and on the boundary of the given region.

Motivated by some recent substantial advances on DRM, Trefftz and MFS, we propose DRM-Trefftz and DRM-MFS models for analysing transient heat conduction problems in this paper. First, the time stepping method is used in handling the time variable of the heat conduction process and then the system is replaced by a set of inhomogeneous modified Helmholtz equations. The solution of the modified Helmholtz equation can be divided into two parts, i.e. the particular solution and the homogeneous solution. The particular solution is solved by DRM in which the source term is approximated by radial basis functions (RBF), while, both the Trefftz method and MFS are employed to construct the homogeneous solution. The paper is organized as follows. The DRM-Trefftz and DRM-MFS models are introduced in Section 2, followed by numerical validations in terms of some 2D transient heat conduction problems in Section 3, and finally, some concluding remarks are presented based on the reported results in Section 4.

## 2. NUMERICAL METHOD AND ALGORITHMS

### 2.1. Basic Formulations of Transient Heat Conduction

Consider a two-dimensional heat conduction equation which models an unsteady temperature distribution in a solid (domain  $\Omega$ ). This problem is governed by the differential equation:

$$k\nabla^2 u(X,t) + Q(X,t) = \rho c \partial u(X,t) / \partial t \quad (1)$$

With the boundary conditions:

- Dirichlet/necessary condition

$$u(X,t) = \bar{u}(X,t) \quad X \in \Gamma_u \quad (2)$$

- Newman/nature condition

$$q(X,t) = \bar{q}(X,t) \quad X \in \Gamma_q \quad (3)$$

- convective condition

$$q(X,t) = h_e [u(X,t) - u_\infty] \quad X \in \Gamma_c \quad (4)$$

And the initial condition

$$u(X,0) = u_0 \quad X \in \Omega \quad (5)$$

where  $u(X,t)$  is the temperature function,  $k$  is the specified thermal conductivity,  $\nabla^2 = \partial^2/\partial x^2 + \partial^2/\partial y^2$  is the two-dimensional operator,  $\rho$  is the mass density,  $c$  is the

specific heat and the overhead bar designates the imposed quantities.  $q$  represents the boundary heat flux defined as  $q = -k\partial u/\partial n$  and  $n$  is the unit outward normal to the boundary  $\Gamma$ . Furthermore,  $u_0$  is the initial temperature,  $h_e$  is the heat transfer coefficient and  $u_\infty$  is the environmental temperature. For a well-posed problem, we have  $\Gamma = \Gamma_u \cup \Gamma_q \cup \Gamma_c$ .

For convenience, boundary conditions (2)-(4) are expressed in a general form as

$$B_1 u(X,t) + B_2 q(X,t) = B_3(X,t) \quad (6)$$

where  $B_1$ ,  $B_2$ , and  $B_3$  are known coefficients and can be written respectively as

$$\begin{cases} B_1 = 1, & B_2 = 0, & B_3 = \bar{u} & \text{on } \Gamma_u \\ B_1 = 0, & B_2 = 1, & B_3 = \bar{q} & \text{on } \Gamma_q \\ B_1 = h_e, & B_2 = -1, & B_3 = h_e u_e & \text{on } \Gamma_c \end{cases} \quad (7)$$

### 2.2. Time-Stepping Scheme

In the literature there are different approaches to handle time variable, two of which are: (1) Laplace transform; (2) finite differencing in time. Since numerical inversion of the Laplace transform is often ill-posed, here we apply the finite difference scheme to handle the time variable. For a typical time interval  $[t^n, t^{n+1}] \subset [0, T]$ ,  $u(X, t)$ , its derivative with respect to time variable  $t$  and  $Q(X, t)$  are approximated as [35]:

$$\begin{aligned} u(X,t) &= \theta u^{n+1}(X) + (1-\theta)u^n(X) \\ \frac{\partial u(X,t)}{\partial t} &= \frac{u^{n+1}(X) - u^n(X)}{\tau} \\ Q(X,t) &= \theta Q^{n+1}(X) + (1-\theta)Q^n(X) \end{aligned} \quad (8)$$

where the superscripts  $n$  and  $n+1$  refer to subsequent time instances and  $\tau = t^{n+1} - t^n$  is the time step size.  $\theta$  ( $0 \leq \theta \leq 1$ ) is a real parameter that determines if the method is explicit ( $\theta = 0$ ), implicit ( $\theta = 1$ ) or a linear combination of both types [36]. The special choice of  $\theta = 1/2$  is known as the Crank Nicolson scheme in the literature.

It is easily verified that the conditions which prevent oscillations in the explicit case are exactly the same as the commonly cited sufficient conditions which ensure that it is stable. Furthermore, even though a Crank Nicolson approach is unconditionally stable, it permits the development of spurious oscillations unless the time step size is no more than twice that required for an explicit method to be stable. Although an implicit scheme is only first-order accurate in time, it is proved that the Partial differential Equation (PDE) can be solved accurately using the implicit scheme [37]. Hence, we use  $\theta = 1$  in our analysis.

Substituting Eq. (8) into Eqs. (1) and (6) and rearranging it yields the following modified Helmholtz-type equation

that has to be solved at each time step  $t^{n+1}$  for the unknown  $u^{n+1}(X)$  :

$$\nabla^2 u^{n+1}(X) - \frac{\rho c}{k\tau} u^{n+1}(X) = -\frac{\rho c}{k\tau} u^n(X) - \frac{1}{k} Q^n(X) \quad (9)$$

$$\left[ B_1 u^{n+1}(X) + B_2 q^{n+1}(X) \right] = B_3^{n+1}(X) \quad (10)$$

Note that the right-hand side of Eq. (9) is well defined in terms of the approximate solution  $u^n$  calculated on the previous time step  $t = t^n$ . To start the procedure we take  $u(X, 0) = u_0$ , the initial condition of the transient problem.

For simplicity, the single step formula Eq. (9) can be written as

$$(\nabla^2 - \lambda^2)u(X) = f(X) \quad (11)$$

where

$$\lambda = \sqrt{\frac{\rho c}{\tau k}} \quad (12)$$

$$f(X) = -\frac{\rho c}{\tau k} u^n(X) - \frac{Q^n(X)}{k} \quad (13)$$

Eq. (11) is a sequence of inhomogeneous modified Helmholtz equation, the solution of which is discussed in the next section.

### 2.3. Implementation of the Proposed Meshless Method

Due to linear property of Eq. (11), its solution can be expressed as a summation of a particular solution  $u_p$  and a homogeneous solution  $u_h$ , that is:

$$u = u_p + u_h \quad (14)$$

where  $u_p$  satisfies the inhomogeneous equation

$$(\nabla^2 - \lambda^2)u_p(X) = f(X) \quad X \in \Omega \quad (15)$$

but does not necessarily satisfy the boundary conditions (2)-(4), and  $u_h$  satisfies:

$$(\nabla^2 - \lambda^2)u_h(X) = 0 \quad X \in \Omega \quad (16)$$

$$\begin{cases} u_h(X, t) = \bar{u}(X, t) - u_p(X, t) & X \in \Gamma_u \\ q_h(X, t) = \bar{q}(X, t) - q_p(X, t) & X \in \Gamma_q \\ h_{\infty} u_h(X, t) - q_h(X, t) = h_{\infty} u_{\infty} - h_{\infty} u_p(X, t) + q_p(X, t) & X \in \Gamma_c \end{cases} \quad (17)$$

Similar to the treatment of Eq. (6), Eq. (17) can be written in a general form:

$$\left[ B_1 u_h(X) + B_2 q_h(X) \right] = B_3(X) \quad (18)$$

#### 2.3.1. Dual Reciprocity Method (DRM) for Particular Solution

The particular solution  $u_p$  can be obtained by DRM. To do this, the right-hand side term of Eq. (15) is approximated by RBF [38], yielding

$$f(X) = \sum_{i=1}^{N_i} \alpha_i \varphi_i(X) \quad X \in \Omega \quad (19)$$

where  $N_i$  is the number of interpolation points in the domain under consideration. Here,  $\varphi_i(X) = \varphi(r) = \varphi(|X - X_i|)$  denotes radial basis functions with the reference point  $X_i$  and  $\alpha_i$  are interpolating coefficients to be determined.

Simultaneously, the particular solution  $u_p$  is similarly expressed as

$$u_p(X) = \sum_{i=1}^{N_i} \alpha_i \psi_i(X) \quad (20)$$

where  $\psi_i$  represent corresponding approximated particular solutions which satisfy the following differential equations:

$$(\nabla^2 - \lambda^2)\psi_i = \varphi_i \quad (21)$$

noting the relation between the particular solution  $u_p$  and function  $f(X)$  in Eq. (15).

By enforcing Eq. (20) to satisfy Eq. (15) at all nodes, we can obtain a set of simultaneous equations to uniquely determine the unknown coefficients  $\alpha_i$ . In this procedure, we need to evaluate the approximate particular solutions in terms of the RBF  $\varphi$ . The standard approach is that  $\varphi$  is first selected, and then the corresponding approximate particular solutions are determined by solving Eq. (21) analytically. For the Laplace operator,  $\psi$  can be obtained by repeated integration, but for the Helmholtz-type operator, this has proven difficult [24, 39]. A significant result for Helmholtz-type operator was given by Chen and Rashed where analytic formulas were given for  $\psi$  when  $\varphi$  as a Thin Plate Spline (TPS) [40]:

$$\varphi = r^2 \ln r \quad (22)$$

$$\begin{cases} \psi(\mathbf{r}) = -\frac{4}{\lambda^4} - \frac{4 \ln r}{\lambda^4} - \frac{r^2 \ln r}{\lambda^2} - \frac{4K_0(\lambda r)}{\lambda^4} & r \neq 0 \\ \psi(\mathbf{r}) = -\frac{4}{\lambda^4} + \frac{4\gamma}{\lambda^4} + \frac{4}{\lambda^4} \ln\left(\frac{\lambda}{2}\right) & r = 0 \end{cases} \quad (23)$$

where  $\gamma \approx 0.5772156649015328$  is Euler's constant.

Another scheme for obtaining approximate particular solutions is a reverse approach [36, 37]. Here,  $\psi$  is first chosen directly and Eq. (22) is used to evaluate  $\varphi$ . For example, the particular solutions  $\psi$  are directly chosen as follows [22]:

$$\psi(\mathbf{r}) = \frac{r^2}{4} + \frac{r^3}{9} \quad (24)$$

and the corresponding  $\varphi$  is obtained as

$$\varphi(\mathbf{r}) = 1 + r - \lambda^2 \left( \frac{r^2}{4} + \frac{r^3}{9} \right) \quad (25)$$

It is difficult to prove mathematically under what conditions this approach is reliable, although it seems to work well so far for many problems [41-43]

An additional polynomial term  $p$  is required to assure nonsingularity of the interpolation matrix if the RBF is conditionally positive definite such as TPS [44, 45]. And also, to achieve higher convergence rates for  $f(X)$ , the higher order splines are considered [46]. For example,

$$\varphi = r^{2n} \ln r \quad n \geq 1, \text{ in } \mathbb{R}^2 \quad (26)$$

Then

$$f(X) = \sum_{i=1}^{N_j} \alpha_i \varphi_i^{[n]}(X) + P_n \quad (27)$$

where  $P_n$  is a polynomial of total degree  $n$  and let  $\{b_j\}_{j=1}^{l_n}$  be a basis for  $P_n$  ( $l_n = \binom{n+d}{d}$  is the dimension of  $P_n$ , and  $d=2$  for a 2 dimension problem). The corresponding boundary conditions are given by

$$\sum_{i=1}^{N_j} \alpha_i b_i(P_j) = 0, \quad 1 \leq l \leq l_n \quad (28)$$

Since the inhomogeneous term  $f(X)$  in Eq. (11) is a known function depending on the temperature field  $u^n$ , the coefficients  $\alpha_i$  can be determined by solving Eq. (11) and Eq. (28). Then the particular solution can be obtained from Eq. (20).

The next step is to solve homogeneous solution  $u_h$ . Here we consider two typical methods — Trefftz method and MFS, which are based on Trefftz solution and fundamental solution, respectively. The details are follows in the next section.

### 2.3.2. Trefftz Function for Homogeneous Solution

Introducing polar coordinates  $(r, \theta)$  with  $r=0$  at the centroid of  $\Omega$ , it is known that the set

$$N = \{I_n(\lambda r) \cos n\theta\}_{n=0}^{\infty} \cup \{I_n(\lambda r) \sin n\theta\}_{n=1}^{\infty} \quad (29)$$

are T-complete solutions of the modified Helmholtz equation, where  $I_n$  is the modified Bessel function of first kind with order  $n$ .

Hence, the homogeneous solution to (16)-(17) is approximated as

$$u_h(X) = \sum_{j=1}^m c_j N_j(X) \quad (30)$$

where  $c_j$  are the coefficients to be determined and  $m$  is its number of components. The terms  $N_j(X) = N(r) = N(|X - X_j|)$  are the T-complete solutions of the modified Helmholtz operator  $(\nabla - \lambda^2)$ , and  $\{X_j\}_{j=1}^{N_s}$  are collocation points placed on the physical boundary of the solution domain. As an illustration, the internal function  $N_j$  in Eq. (30) can be given in the form

$$N_1 = I_0(\lambda r), N_2 = I_1(\lambda r) \cos \theta, N_3 = I_1(\lambda r) \sin \theta, \dots, \quad (31)$$

So, Eq. (30) can be written as

$$u_h(X) = \sum_{n=0}^k \alpha_n I_n(\lambda r) \cos n\theta + \sum_{n=1}^k \beta_n I_n(\lambda r) \sin n\theta \quad (32)$$

where  $m = 2k + 1$ . Noted that  $u_h$  in Eq. (30) and (32) automatically satisfies the given differential equation (16), all we need to do is to enforce  $u_h$  to satisfy the modified boundary conditions (17) as  $u_p$  has already been calculated separately. To do this, collocation points  $\{X_j\}_{j=1}^{N_s}$  are placed on the physical boundary to fit the boundary condition (18). It leads to a system of linear algebraic equations in matrix form:

$$[A]_{N_s \times m} \{c\}_{m \times 1} = \{b\}_{N_s \times 1} \quad (33)$$

with

$$\{c\} = \{\alpha_0, \alpha_1, \dots, \alpha_k, \beta_1, \dots, \beta_k\}, \{b\} = \{b_1, b_2, \dots, b_{N_s}\} \quad (34)$$

If the number of components equals to the number of collocation points on the physical boundary ( $m = N_s$ ), this leads to properly determined equations. Alternatively, in case the number of components is smaller than the number of collocation points ( $m < N_s$ ), this results in over-determined equations. The least square method can be used to solve the over-determined equations. Once  $\{c\}$  is obtained,  $u_h$  can be computed at any location in the domain using Eq. (30).

### 2.3.3. MFS for Homogeneous Solution

In the implementation of MFS, the homogeneous solution is approximated in a standard collocation fashion

$$u_h(X) = \sum_{j=1}^{N_s} \beta_j u_j^*(X) \quad (35)$$

where  $\beta_j$  are the coefficients to be determined. The terms  $u_j^*(X) = u^*(r) = u^*\left(\left|X - X_j\right|\right)$  are the fundamental solutions of the modified Helmholtz operator  $(\nabla - \lambda^2)$ . Here the source points  $\{X_j\}_{j=1}^{N_s}$  are placed outside the solution domain.

Typically, for a two-dimensional problem, the fundamental solution is

$$u_j^*(X) = \frac{1}{2\pi} K_0(\lambda r) \quad (36)$$

where  $K_0$  is the modified Bessel function of the second kind with order zero.

For the same reason,  $u_h$  in Eq. (30) automatically satisfies the given differential equation (16), we need to enforce  $u_h$  to satisfy the modified boundary conditions (18) as we did in Trefftz method. But unlike the Trefftz method, MFS needs source points placed outside the solution domain to avoid singularity. In addition, the same number collocation points on the physical boundary are chosen to fit the boundary condition (18). As before, it leads to a system of linear algebraic equations in matrix form:

$$[A]_{N_s \times N_s} \{\beta\}_{N_s \times 1} = \{b\}_{N_s \times 1} \quad (37)$$

With

$$\{\beta\} = \{\beta_1 \beta_2 \dots \beta_{N_s}\}, \quad \{b\} = \{b_1 b_2 \dots b_{N_s}\} \quad (38)$$

Once  $\{\beta\}$  is obtained,  $u_h$  can be computed at any location in the domain using Eq. (35).

Additionally, the generation of source points outside the domain is a curious problem, which affects the accuracy and stability. Generally, the accuracy of the approximation improves as the distance between the virtual and physical boundaries increase. At the same time, the MFS equations can become highly ill-conditioned at this circumstance [38]. At present, there is no uniform approach to generate these source points properly. In our work, a strategy is employed [18]:

$$Y_j = X_j + \gamma(X_j - X_c) \quad (39)$$

where  $X_j$  are boundary nodes,  $X_c$  is the geometric center of the domain and  $\gamma$  is a dimensionless parameter which is arbitrarily chosen as 1.2 for the outer boundary.

### 2.3.4. The Construction of the Solution System

Based on above operations, the complete solution  $u(X)$  for the modified Helmholtz equation can be written as

$$u(X) = \sum_{i=1}^{N_t} \alpha_i \psi_i(X) + \sum_{j=1}^m c_j N_j(X) \quad X \in \Omega \quad (40)$$

For the DRM-Trefftz method, and

$$u(\mathbf{x}) = \sum_{i=1}^{N_t} \alpha_i \psi_i(\mathbf{x}) + \sum_{j=1}^{N_s} \beta_j u_j^*(\mathbf{x}) \quad X \in \Omega \quad (41)$$

For the DRM-MFS method.

Furthermore, the normal heat flux can be obtained as

$$q(X) = -\frac{\partial u(X)}{\partial n} = -\sum_{i=1}^{N_t} \alpha_i \frac{\partial \psi_i(X)}{\partial n} - \sum_{j=1}^m c_j \frac{\partial N_j(X)}{\partial n} \quad X \in \Omega \quad (42)$$

For the DRM-Trefftz method, and

$$q(X) = -\frac{\partial u(X)}{\partial n} = -\sum_{i=1}^{N_t} \alpha_i \frac{\partial \psi_i(X)}{\partial n} - \sum_{j=1}^{N_s} \beta_j \frac{\partial u_j^*(X)}{\partial n} \quad X \in \Omega \quad (43)$$

For the DRM-MFS method. Above is the basic idea of the proposed methods, we will give some numerical examples in the following section.

## 3. NUMERICAL EXAMPLES

In order to demonstrate the efficiency and accuracy of the proposed meshless method and the selected RBF and virtual boundary, two benchmark numerical examples of transient heat conduction problems are considered for which corresponding exact solutions are known and can be used for verification. The domain in these two examples is a  $3 \times 3$  square. In the computation,  $\rho c = 1, k = 1.25, Q = 0$  are assumed. The third example is more complicated with non-smooth boundary.

In addition, to provide a quantitative understanding of the results, the average relative error on a variable  $f$  is introduced as

$$Arerr(f) = \sqrt{\frac{\sum_{i=1}^N (f_{numerical} - f_{exact})_i^2}{\sum_{i=1}^N (f_{exact})_i^2}} \quad (44)$$

where  $N$  is the number of test points and  $(f)_i$  is an arbitrary field function, such as a temperature at point  $i$ .

**Example 1:** Consider a classic heat diffusion problem which has been studied using the finite element method by Bruch and Zyvoloski [7], BEM with time-dependent fundamental solutions by Brebbia and Wroble [8], DRBEM by Partridge [13] and Trefftz finite element method by Jirousek and Qin [9]. The initial temperature of the whole domain is  $30^\circ$  and cooled by the application of a thermal shock ( $u = 0^\circ \text{C}$  all over the boundary), the geometry and boundary conditions of the problem are shown in Fig. (1).

$$u(0, y, t) = u(x, 0, t) = u(3, y, t) = u(x, 3, t) = 0, \quad u_0(x, y) = 30^\circ$$

The analytical solution of this problem is

$$u(x, y, t) = \sum_{n=0}^{\infty} \sum_{j=0}^{\infty} A_n \sin \frac{n\pi x}{3} \sin \frac{j\pi y}{3} \times \exp\left[-\frac{k\pi^2(n^2 + j^2)t}{3^2}\right]$$

where

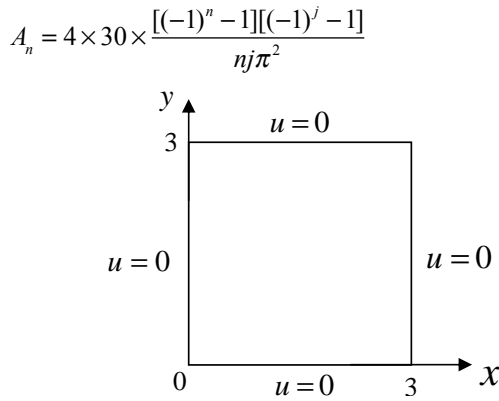


Fig. (1). Geometry of square domain and boundary conditions for example 1.

In order to investigate the effect of the component number  $m$  in Eq. (30), the number of components is chosen as 10, 20, 30 and 40, respectively, and 40 collocation points in the calculation. It can be seen from Fig. (2) that the results gradually converge to the exact values as the number of components ( $m$ ) increases. This can be explained by that the least square method can achieve better numerical accuracy in solving the over-determined equations when the number of unknowns is close to the number of equations. But, from Fig. (2) we also observe that a larger  $m$  leads to a larger condition number of matrix A, which is not beneficial to some complex problem. So, the optimal value of  $m$  should be found by numerical experimentation. The value of  $m$  is taken to be the same as the number of collocation points on the boundary in the following numerical simulation.

Table 1 presents the results obtained by DRM-Trefftz and DRM-MFS and other solutions, obtained with the same value of time step ( $\tau = 0.05$ ). For the sake of comparison, the same space discretization as in Ref. [13] is employed. It should be mentioned that the difference between BEM1 and BEM2 in Table 1 is as follows [8]: with BEM1, internal cells were employed in order to account for the initial conditions at the beginning of each time step, while for BEM2, the solution process always restarted at the initial time and domain discretization was avoided. It can be seen clearly from Table 1 that the results obtained by proposed meshless methods (DRM-Trefftz and DRM-MFS) agree well with the exact solution and appear to be more accurate than the results obtained from other methods.

Table 1. Comparison of Results at  $t = 1.2$

Point	x	y	DRM-Trefftz	DRM-MFS	BEM1 [8]	BEM2 [8]	FEM [7]	DRBEM [13]	Trefftz FEM [9]	Exact
1	2.4	1.5	1.0263	1.0263	1.114	1.122	1.139	1.099	1.103	1.065
2	2.4	2.4	0.5985	0.5985	0.657	0.663	0.670	0.645	0.660	0.626
3	1.8	1.5	1.6868	1.6868	1.798	1.809	1.843	1.784	1.797	1.723
4	1.8	1.8	1.6022	1.6022	1.713	1.721	1.753	1.695	1.715	1.639
5	1.5	1.5	1.7760	1.7760	1.887	1.902	1.938	1.877	1.894	1.812

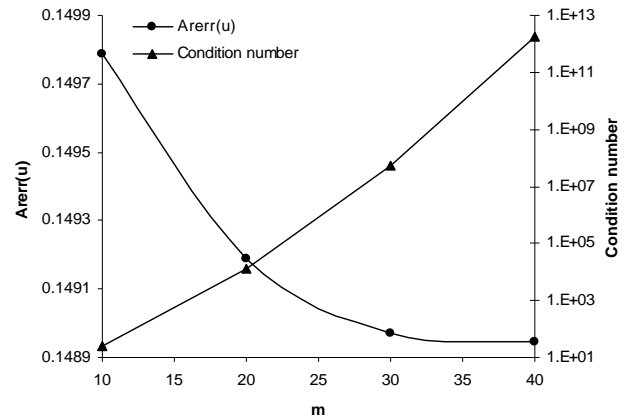


Fig. (2). Effect of various component number to numerical accuracy and condition number of matrix A.

The error in the meshless methods can be split into two parts: one is due to approximating homogeneous solutions and the other is due to approximating particular solutions. One phenomenon that should be noticed is that the two meshless methods we proposed converge to the same value. Since the same RBF is used to approximate particular solutions for both DRM-Trefftz and DRM-MFS, it indicates that Trefftz bases and MFS make the same contribution to the error of the homogeneous part. That means, using Trefftz bases and fundamental solution to approximate homogeneous solutions can achieve the same accuracy. So, DRM plays a very important role in the convergent behaviour of the meshless methods. In order to evaluate the efficiency of DRM, we employ different RBF (standard method and reverse method) in DRM for assessment. Moreover, for standard approach, splines with different order are considered. In Table 2,  $Si$  ( $i = 1-4$ ) denote the results gained by using splines  $\varphi = r^{2i} \ln r$  in Eq. (19) and without additional polynomial term ( $\tau = 0.05$ ). For comparing purpose,  $PSi$  ( $i = 1-4$ ) denote the results gained by using Eq. (27) with additional polynomial terms  $P_i$ .

The numerical results in Table 2 show that the use of higher-order RBF interpolation functions does not improve computing accuracy in transient problems. A previous work [46] showed that more accurate results can be obtained by using higher order polyharmonic splines for elliptic boundary value problems, but from the above results we can see limited improvement for time-dependent problems, presumably because the dominant error was caused by the

**Table 2. Comparison of Results By Different RBF in DRM ( $t = 1.2$ )**

Point	S1	S2	S3	S4	S5	PS1	PS2	PS3	PS4	PS5	Reverse Method	Exact
1	1.048	1.119	1.118	1.204	1.021	1.034	1.104	1.137	1.157	1.158	1.026	1.065
2	0.611	0.658	0.649	0.720	0.560	0.599	0.642	0.668	0.681	0.680	0.599	0.626
3	1.721	1.817	1.820	1.933	1.686	1.703	1.797	1.841	1.871	1.874	1.687	1.723
4	1.635	1.728	1.730	1.840	1.599	1.618	1.708	1.751	1.779	1.782	1.602	1.639
5	1.812	1.910	1.914	2.031	1.777	1.793	1.890	1.936	1.967	1.971	1.776	1.812

time-stepping scheme. Moreover, the higher-order polyharmonic splines result in worse conditioning of the linear system associated with the homogeneous solution. Therefore, care must be taken in using higher-order RBFs. It can be seen from the results that when the order  $i$  is even ( $i = 2, 4$ ), adding additional polynomial terms can increase the accuracy, but when the order  $i$  is odd ( $i = 1, 3, 5$ ), the results are opposite. The reverse method is more accurate than the standard method except for  $i = 1$  (S1, PS1). Moreover, the reverse method can save a lot of computing time without calculating modified Bessel functions which is quite complex and really time consuming. Therefore, the reverse method is employed in the following computation.

Fig. (3) shows the absolute error of temperature for two different time steps. It can be seen that the smaller the time step is, the greater is the accuracy of the results obtained. But more computational time will be required when a smaller time step is employed. Additionally, further reduction in the time step does not reduce the error [47].

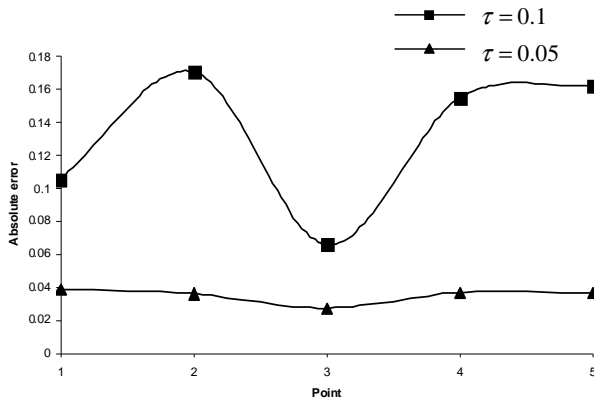


**Fig. (3).** Effect of time step on absolute error of temperature.

**Example 2:** The second example differs from the previous one only by the boundary conditions, which is shown in Fig. (4).

$$u(x, 0, t) = u(3, y, t) = u(x, 3, t) = 0, \partial u(0, y, t) / \partial x = 0$$

$$\text{and } u_0(x, y) = 30$$

The analytical solution of this problem is

$$u(x, y, t) = \sum_{n=0}^{\infty} \sum_{j=0}^{\infty} B_n \sin \frac{(2n-1)\pi x}{2 \times 3} \sin \frac{j\pi y}{3} \times \exp \left[ \frac{-k\pi^2 ((n-0.5)^2 + j^2)t}{3^2} \right]$$

where

$$B_n = 8 \times 30 \times (-1)^{n+2} \frac{(-1)^j - 1}{j\pi^2(2n-1)}$$

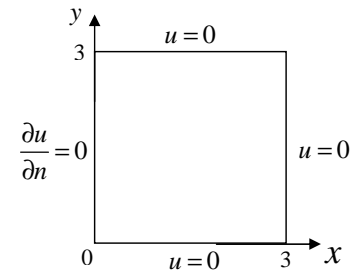


**Fig. (4).** Geometry of square domain and boundary conditions for example 2.

Table 3 presents the results obtained by DRM-Trefftz and DRM-MFS and comparison is made with other solutions, such as FEM and Trefftz FEM, obtained with the same time step value ( $\tau = 0.05$ ). As expected, there is almost no difference among the two meshless methods and their results agree well with the exact solutions. Again, the proposed method can achieve more accurate results than those from other numerical methods.

**Example 3:** The heat conduction problems in engineering or space technology are often complicated because of the complex geometry. In order to test the method for a domain with non-smooth boundary we consider a L-shaped domain (see Fig. 5). 80 source points are placed outside the domain, the same number of collocation points on the boundary and 261 domain interpolation points are employed in the domain for RBF-MFS method (see Fig. 6). In the following iterative procedure,  $t=1$  and iterative number  $N=50$ , and  $\tau = 0.02$  are used. The analytic solutions are the function of time and position of the points:  $u(x, t) = \cos(3x_1) \sinh(2x_2) \exp(-5t)$  [48]. Fig. (7) shows the temperature history at the points of interest A and B, respectively. It can be seen that the solutions obtained by the two numerical methods agree well with each other and converge to the analytical solution as time increases.

In addition, to investigate the effect of the number of collocation points on convergent performance of the model, different numbers of collocation points on the boundary (20, 40, 60, 80) are employed in the calculation. From previous analysis, we know that both DRM-MFS and DRM-Trefftz can converge to the analytical solution, so the calculation is just performed using RBF-MFS only. The convergent

**Table 3. Comparison of Results from Various Methods at  $t = 1.2$**

Point	x	y	DRM-Trefftz	DRM-MFS	FEM [7]	Trefftz FEM [9]	Exact
1	1.5	0.3	1.3780	1.3779	1.418	1.393	1.377
2	1.5	0.6	2.6179	2.6719	2.697	2.615	2.618
3	1.5	0.9	3.6002	3.6001	3.713	3.649	3.604
4	1.5	1.2	4.2332	4.2332	4.364	4.298	4.237
5	1.5	1.5	4.4519	4.4519	4.589	4.524	4.455

numerical results obtained at  $t = 1s$  are compared with the analytical solution. Table 4 shows the average relative error for the whole domain. It can be seen that more collocation points are used, more accurate results can be achieved.

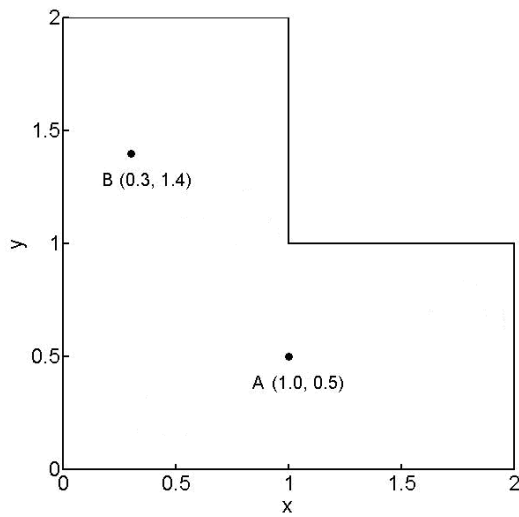


**Fig. (5).** Domain's geometry with locations of the points of interest.

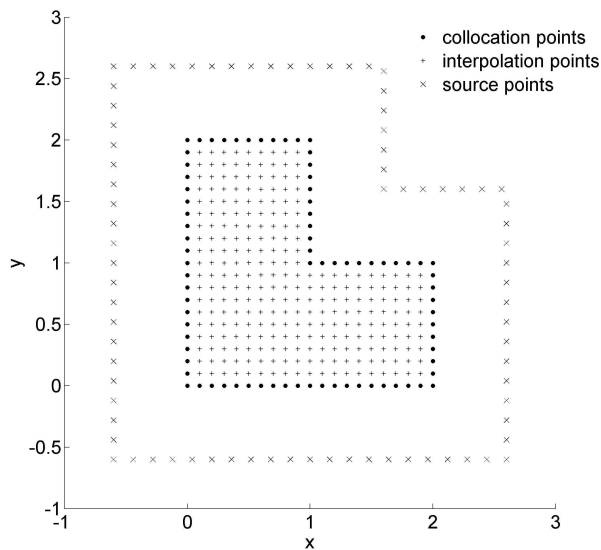


**Fig. (6).** Demonstration of source points, collocation and interpolation points.

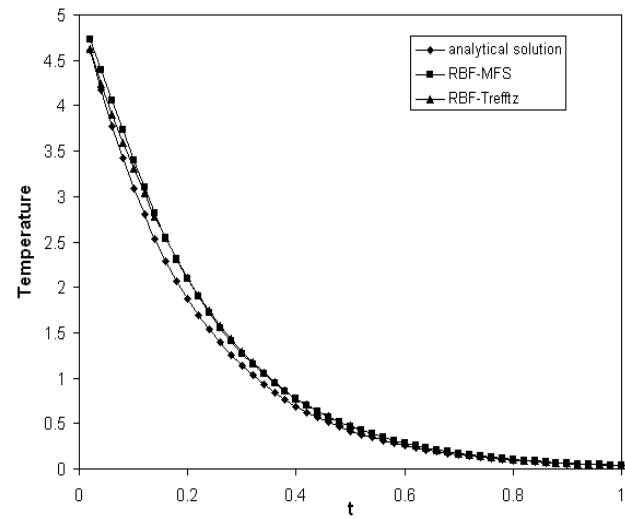
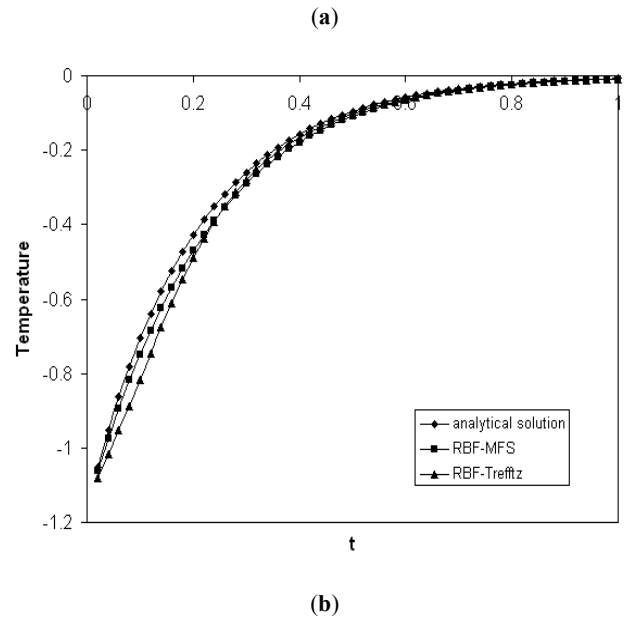


**Fig. (7).** (a) Temperature history at point A (b) Temperature history at point B.

**Table 4. Effect of the Number of Collocation Points on Accuracy**

Number of Collocation Points	20	40	60	80
Arerr	2.18E-1	1.21E-1	1.19E-1	1.18E-1

## CONCLUSION

Two new meshless approaches for solving transient heat conduction problems are developed. Both of the algorithms use DRM to solve the particular solution. The homogeneous solution is approximated by linear combination of Trefftz bases in DRM-Trefftz while by linear combination of fundamental solution in DRM-MFS. It should be mentioned that using Trefftz bases and fundamental solution can achieve the same accuracy for solving homogeneous solution. Among the two methods, DRM-Trefftz is easier to implement since it is non-singular, so it is unnecessary to place source points outside the domain for avoiding singularity which does occur in DRM-MFS. Finally, numerical results show clearly that the methods presented can achieve very high accuracy when compared to other conventional numerical methods. Furthermore, the methods described in this paper can easily be extended to three-dimensional problems and nonlinear problems. This work is underway.

## NOTATIONS

$c$	=	Specific heat (J/kg/ °C)
$h_{\infty}$	=	Conventional coefficient (W/m <sup>2</sup> / °C)
$k$	=	Thermal conductivity (W/m/ °C)
$Q$	=	Spatial heating (W/m <sup>3</sup> )
$q$	=	Normal heat flux (W/m <sup>2</sup> )
$t$	=	Time (s)
$u$	=	Temperature (°C)
$u_0$	=	Initial temperature (°C)
$u_{\infty}$	=	Environmental temperature (°C)
$N_1$	=	Number of interpolation points in the domain
$N_s$	=	Number of source points outside the domain
$m$	=	Number of components for T-complete solution

## GREEK SYMBOLS

$\lambda$	=	Frequency of the modified Helmholtz equation
$\alpha$	=	Interpolating coefficient defined in Eq. (19)
$\beta$	=	Interpolating coefficient defined in Eq. (35)
$\gamma$	=	Euler's constant
$\tau$	=	Time step size
$\rho$	=	Density (kg/m <sup>3</sup> )
$\theta$	=	Temporal weighting in time-stepping method

## REFERENCES

- [1] Hidayetoglu TK. Functionally graded friction material. US Patent 7033663, 2000.
- [2] Burris KW, Beardsley BM, Chuzhoy L. Component having a functionally graded material coating for improved performance. US Patent 6087022, 2000.
- [3] Rabiei A. Functionally graded biocompatible coating and coated implant. US Patent 20090304761, 2009.
- [4] Renner E. Thermal engine. US Patent 3937019, 1976.
- [5] Knowles G, Bird RW. Solid state engine with alternating motion. US Patent 20046834835, 2004.
- [6] Brian PLT. A finite-difference method of high-order accuracy for the solution of three-dimensional transient heat conduction problems. *AIChE J* 1961; 7: 367-70.
- [7] John C, Bruch J, George Z. Transient two-dimensional heat conduction problems solved by the finite element method. *Int J Numer Methods Eng* 1974; 8: 481-94.
- [8] Brebbia CA, Telles JCF, Wrobel LC. Boundary element techniques. Suhrkamp Verlag: Springer 1984.
- [9] Jirousek J, Qin QH. Application of hybrid-trefftz element approach to transient heat conduction analysis. *Comput Struct* 1996; 58: 195-201.
- [10] Jutta B, Bialecki RA, Günther K. Transient non-linear heat conduction-radiation problems - a boundary element formulation. *Int J Numer Methods Eng* 1999; 46: 1865-82.
- [11] Wang H, Qin QH, Kang YL. A meshless model for transient heat conduction in functionally graded materials. *Comput Mech* 2006; 38: 51-60.
- [12] Mansur WJ, Brebbia CA. Formulation of the boundary element method for transient problems governed by the scalar wave equation. *Appl Math Model* 1982; 6: 307-311.
- [13] Partridge PW, Brebbia CA, Wrobel LC. The dual reciprocity boundary element method. Computational mechanics publications. London: Southampton and Elsevier Applied Science 1992.
- [14] Bulgakov V, Scaronarler B, Kuhn G. Iterative solution of systems of equations in the dual reciprocity boundary element method for the diffusion equation. *Int J Numer Methods Eng* 1998; 43: 713-32.
- [15] Singh KM, Tanaka M. Dual reciprocity boundary element analysis of nonlinear diffusion: Temporal discretization. *Eng Anal Bound Elem* 1999; 23: 419-33.
- [16] Bialecki RA, Jurgas P, Kuhn G. Dual reciprocity bem without matrix inversion for transient heat conduction. *Eng Anal Bound Elem* 2002; 26: 227-36.
- [17] Nowak AJ, Brebbia CA. The multiple-reciprocity method. A new approach for transforming bem domain integrals to the boundary. *Eng Anal Bound Elem* 1989; 6: 164-7.
- [18] Young DL, Jane SJ, Fan CM, Murugesan K, Tsai CC. The method of fundamental solutions for 2d and 3d stokes problems. *J Comput Phys* 2006; 211: 1-8.
- [19] Smyrliis YS, Karageorghis A. Some aspects of the method of fundamental solutions for certain harmonic problems. *SIAM J Sci Comput* 2001; 16: 341-71.
- [20] Fairweather G, Karageorghis A. The method of fundamental solutions for elliptic boundary value problems. *Adv Comput Math* 1998; 9: 69-95.
- [21] Chen CS, Golberg MA, Hon YC. The method of fundamental solutions and quasi-monte-carlo method for diffusion equations. *Int J Numer Methods Eng* 1998; 43: 1421-35.
- [22] Balakrishnan K, Sureshkumar R, Ramachandran PA. An operator splitting-radial basis function method for the solution of transient nonlinear poisson problems. *Comput Math Appl* 2002; 43: 289-304.
- [23] Golberg MA, Chen CS, Bowman H, Power H. Some comments on the use of radial basis functions in the dual reciprocity method. *Comput Mech* 1998; 21: 141-8.
- [24] Golberg M, Chen CS. The theory of radial basis functions applied to the bem for inhomogeneous partial differential equations. *Bound Elem Commun* 1994; 5: 57-61.
- [25] Koopmann GH, Song L, Fahline JB. A method for computing acoustic fields based on the principle of wave superposition. *J Acoust Soc Am* 1989; 86: 2433-8.
- [26] Amano K. A charge simulation method for the numerical conformal mapping of interior, exterior and doubly-connected domains. *J Comput Appl Math* 1994; 53: 353-70.
- [27] Wang H, Qin QH, Kang YL. A new meshless method for steady-state heat conduction problems in anisotropic and inhomogeneous media. *Arch Appl Mech* 2005; 74: 563-79.
- [28] Trefftz E. Ein gegenstück zum ritzschen verfahren. Proceedings of 2nd International Conference of Applied Mechanics, Zurich, Switzerland 1926; pp. 131-7.
- [29] Jin WG, Cheung YK, Zienkiewicz OC. Application of the trefftz method in plane elasticity problems. *Int J Numer Methods Eng* 1990; 30: 1147-61.
- [30] Cheung YK, Jin WG, Zienkiewicz OC. Direct solution procedure for solution of harmonic problems using complete, non-singular, trefftz functions. *Commun Appl Numer Methods* 1989; 5: 159-69.

- [31] Zielinski AP. On trial functions applied in the generalized trefftz method. *Adv Eng Softw* 1995; 24: 147-55.
- [32] Qin QH. Trefftz finite element method and its applications. *Appl Mech Rev* 2005; 58: 316-37.
- [33] Qin QH. Trefftz finite and boundary element method. Southampton: WIT Press 2000.
- [34] Kita E, Ikeda Y, Kamiya N. Trefftz solution for boundary value problem of three-dimensional poisson equation. *Eng Anal Bound Elem* 2005; 29: 383-90.
- [35] Chapko R, Kress R. Rothe's method for the heat equation and boundary integral equations. *J Integral Equ Appl* 1997; 9: 47-69.
- [36] Thomas JW. Numerical partial differential equations illustrated ed. USA: Springer 1995.
- [37] Zvan R, Vetzal KR, Forsyth PA. Pde methods for pricing barrier options. *J Econ Dyn Control* 2000; 24: 1563-90.
- [38] Golberg M. Recent developments in the numerical evaluation of particular solutions in the boundary element method. *Appl Math Comput* 1996; 75: 91-101.
- [39] Golberg M, Chen CS, Fromme J. Discrete projection methods for integral equations. Computational Mechanics Publications: Southampton 1997.
- [40] Chen CS, Rashed YF. Evaluation of thin plate spline based particular solutions for helmholtz-type operators for the drn. *Mech Res Commun* 1998; 25: 195-201.
- [41] Wrobel LC, DeFigueiredo DB. A dual reciprocity boundary element formulation for convection-diffusion problems with variable velocity fields. *Eng Anal Bound Elem* 1991; 8: 312-9.
- [42] Schclar NA. Anisotropic analysis using boundary elements (topics in engineering) (hardcover). UK: WIT Press 1994.
- [43] Kogel M, Gaul L. Dual reciprocity boundary element method for three-dimensional problems of dynamic piezoelectricity. *Eng Anal Bound Elem* 1999; 8: 312-9.
- [44] Kansa EJ. Multiquadrics--a scattered data approximation scheme with applications to computational fluid-dynamics--ii solutions to parabolic, hyperbolic and elliptic partial differential equations. *Comput Math Appl* 1990; 19: 147-61.
- [45] Zerroukat M, Power H, Chen CS. A numerical method for heat transfer problems using collocation and radial basis function. *Int J Numer Methods Eng* 1998; 42: 1263-78.
- [46] Muleshkov AS, Golberg MA, Chen CS. Particular solutions of helmholtz-type operators using higher order polyhrmonic splines. *Comput Mech* 1999; 23: 411-9.
- [47] Schaback R. Error estimates and condition numbers for radial basis function interpolation. *Adv Comput Math* 1995; 3: 251-64.
- [48] Valtchev SN. Roberty, A time-marching MFS scheme for heat conduction problems. *Eng Anal Bound Elem* 2008. 32(6): 480-93.

---

Received: December 4, 2009

Revised: December 16, 2009

Accepted: January 11, 2010

© Qinghua Qin; Licensee *Bentham Open*.

This is an open access article licensed under the terms of the Creative Commons Attribution Non-Commercial License (<http://creativecommons.org/licenses/by-nc/3.0/>) which permits unrestricted, non-commercial use, distribution and reproduction in any medium, provided the work is properly cited.